Geografia-Malaysian Journal of Society and Space 22 issue 2 (16-30)
 https://doi.org/10.17576/geo-2026-2202-02

Quantifying the effects of present and future LULC dynamics on landslide susceptibility: A case study of Idukki District (2021-2050)

Laxmi Ch. N. V., Kumari K. P

School of Spatial Information Technology, IST, JNTUK

Correspondence: Laxmi Ch. N. V (email: lakshmichitikela@gmail.com)

Received: 9 January 2026; Accepted: 1 March 2026; Published: 21 May 2026

Abstract

Land use and land cover (LULC) changes represent significant anthropogenic factors affecting slope stability in mountainous regions. This study examines the impact of LULC changes from 2021 to 2050 on Landslide Susceptibility Mapping (LSM) in the Idukki district by employing Remote Sensing, Geographic Information System (GIS), and statistical modelling. Initially, a spatial geodatabase of nineteen conditioning parameters and historical landslide events was developed. Subsequently, the existing LULC (2021) and projected LULC (2050) were generated using an Artificial Neural Network (ANN)-based Cellular Automata Model. Finally, a future LSM was forecasted using conditioning factors, landslide inventory data, and future LULC through the Frequency Ratio (FR) model. The simulated results indicated a significant increase in the built-up area (4.46%) and a reduction in bare ground (3.22%), with the predicted future LS results showing a 26% rise in the Very High LS zone. These findings hold substantial implications for regional planning in hazard-prone areas, and reforestation measures to mitigate slope instability for disaster risk reduction in the study area.

Keywords: ANN, Frequency Ratio Model, GIS, landslide susceptibility, land use and land cover, Remote Sensing

Introduction

Landslides are among the most destructive natural hazards in mountainous regions worldwide, causing an estimated 55,997 fatalities between 2004-2016 alone (Froude & Petley, 2018). In India, they account for significant losses in the western Ghats. For instance, the 2018 Kerala floods & landslides resulted in over 483 deaths and thousands of affected structures, with Idukki district experiencing 143 major landslides (Martha et al., 2019). These events often lead to considerable loss of life, damage to infrastructure, and long-term socioeconomic disruption (Ajin et al., 2022; Tyagi et al., 2023; Youssef et al., 2022). While natural factors, such as rainfall, geology, and slope gradient, largely govern landslide occurrence, human-induced modifications of land use and land cover (LULC) significantly intensify landslide hazards (Bernardie et al., 2021; Chen et al., 2019; El Jazouli et al., 2019; Guns & Vanacker, 2013). Changes in landuse landcover significantly contribute to reducing slope stability in mountainous regions by altering the hydrological and geotechnical properties of terrain (Leta et al., 2021; Pacheco Quevedo et al., 2023; Yono et al.,

2025). These changes include the expansion of built-up areas, conversion of forest to agriculture fields, and construction on unstable slopes.

Traditional Landslide Susceptibility Mapping (LSM) often relies on static conditioning factors and neglects the role of evolving LULC. However, landscapes are dynamic, and future risk assessments require scenario-based estimations that account for projected LULC changes (Chowdhuri et al., 2021; Li et al., 2024; Roccati et al., 2021; Sharma & Sandhu, 2024). This study addresses this gap by analyzing how present and future land cover patterns influence landslide susceptibility, focusing on quantifiable shifts between 2021 and 2050.

Literature review

In 2020, the study area was predominantly covered by tree canopy, accounting for 3,522.83 km² (approximately 70.4% of the total area), indicating a largely forested landscape. Bare ground followed as the second-largest class, covering 957.65 km² (19.1%), while built-up areas occupied 361.59 km² (7.2%). Water bodies spanned 118.41 km² (2.4%), with minor contributions from crops (37.92 km², 0.8%) and flooded vegetation (6.16 km², 0.1%). These conditions reflect a semi-rural to forested region in Idukki, where natural vegetation dominates but is increasingly pressured by human activities. Between 2020 and 2021, the extent of built-up areas increased by 6.36 km², representing a 1.76% growth relative to the 2020 baseline. This expansion was largely driven by deforestation, with tree cover decreasing by 5.56 km² (a 0.16% reduction) and bare ground declining by 6.73 km² (0.70% reduction). Conversely, crops and flooded vegetation saw gains of 2.29 km² (6.04% increase) and 2.07 km² (33.60% increase), respectively, while water bodies expanded slightly by 1.62 km² (1.37%) shown in Table 2. These changes suggest land-use conversions primarily from trees and bare ground to built-up or agricultural areas, exacerbating habitat fragmentation in the study region

Several studies have investigated the relationship between land use/land cover (LULC) changes and landslide susceptibility in the state of Kerala, India. Hao et al. (2022) examined how land-use modifications contributed to the devastating 2018 landslides, highlighting Idukki as a critical hotspot. This aligns with related studies on landslide susceptibility in the area such as (Jacinth Jennifer & Saravanan, 2022) on ANN based mapping and (Jones et al., 2021) on regression and machine learning approaches. Achu et al. provided a statewide analysis of landslide susceptibility under extreme rainfall, reporting that nearly 13% of Kerala is highly prone to slope failures. At the district level, studies in Idukki quantified the impact of built-up expansion on slope instability, whereas case-specific assessments in Wayanad and Kozhikode applied GIS and machine learning techniques to delineate Landslide Susceptibility Zones (LSZs). These studies collectively emphasize that deforestation, agricultural expansion, and unplanned urban growth significantly increase the landslide risk (Bozzolan et al., 2023; Muñoz-Torrero Manchado et al., 2022; P et al., 2025).

However, most of these studies relied on present or past LULC conditions, focusing on either single events (such as the 2018 disaster) or static susceptibility mapping. Few attempts have been made to incorporate future LULC scenarios into landslide modeling, which is crucial for understanding how projected land-cover transformations may alter hazard dynamics (Achu et al., 2021; Dixit et al., 2022). In particular, despite being one of the most landslide-prone areas in Kerala, with frequent slope failures affecting hydropower infrastructure, agriculture, and settlements, a forward-looking, scenario-based susceptibility assessment is still lacking. The FR

model was selected as the primary method for several key reasons aligned with the study's objectives and constraints.FR offers interpretability and simplicity, allowing direct quantification of each conditioning factor's relative influence through ratio values, which is particularly valuable for stakeholders in disaster management who may not have expertise in complex ML black-box models.

In this study, we addressed this gap by developing Landslide Susceptibility Maps (LSMs) for 2021 and for a projected LULC scenario in 2050. By isolating the effect of LULC change while keeping other conditioning factors constant, we evaluated how human-induced landscape transformations are likely to influence slope stability in the coming decades. This approach not only advances the methodological framework of LSM but also provides decision-makers with anticipatory insights for sustainable land management in Kerala's most vulnerable regions (Ramachandran & Reddy, 2017).

Method and study area

The study zone encompasses the Idukki district (longitude 76°.62′, 77°.41′, latitude 9°.27′, 10°.35′) of Kerala, covering an area of 5004.55 km^2 Figure 1 (Laxmi & Kumari, 2024). The study area is characterized by diverse topography (Anchima et al., 2023), ranging from lush green valleys to steep slopes. It is home to a rich variety of flora and fauna, making it a biodiversity hotspot of global significance. Notable flora includes over 1,800 flowering plant species, with endemics such as Neelakurinji (Strobilanthes kunthiana)-famous for its periodic mass blooming and shola forest trees like Mesua indica and Syzygium spp., alongside tropical evergreen and semi-evergreen forests that provide critical root reinforcement for soil stability and erosion control. Fauna features endangered endemics like the Nilgiri Tahr (Nilgiritragus hylocrius), alongside Asian Elephant (Elephas maximus), Gaur (Bos gaurus), Sambar Deer (Rusa unicolor), Nilgiri Langur, and diverse avifauna including the Malabar Grey Hornbill, highlighting its importance for conservation and sustainable development (Abraham et al., 2019; Chitikela & Kollipara, 2025; Suriyankietkaew et al., 2025).

The LULC changes from 2020 to 2021 reveal varied dynamics across classes, Built-up areas experienced the largest absolute gain (+6.36 km²), translating to a 1.76% increase in coverage. Flooded vegetation showed the most significant relative growth at 33.61% (+2.07 km²), likely due to seasonal flooding or wetland expansion. Crops increased by 6.04% (+2.29 km²), indicating agricultural intensification. Water bodies grew modestly by 1.37% (+1.62 km²). In contrast, trees and bare ground declined by 0.16% (-5.56 km²) and 0.70% (-6.73 km²), respectively. These one-year shifts represent an initial trend toward urbanization and habitat loss, with a net loss of 12.29 km² in natural cover (trees + bare ground) in Table 2. The short-term percentage changes from 2020 to 2021 serve as initial indicators of land-use dynamics but are not directly extrapolated for long-term projections due to potential anomalies.

Annual rainfall of idukki, ranging from 2,500 to 3,800 mm, primarily due to the southwest monsoon from June to September (70–80% of total), is more abundant at higher altitudes and is unevenly distributed across the region. Rainfall intensity often exceeds 50–100 mm/hour in convective storms, while event duration typically spans 3–5 days for major episodes, leading to cumulative precipitation of 200–500 mm per event thresholds known to saturate lateritic soils and trigger landslides in steep terrains. Extreme events are frequent; for instance, the 2018 Kerala

floods saw Idukki receive over 1,000 mm in a week (peak daily intensity ~200–300 mm), far surpassing the IMD's very heavy rain threshold (124.5 mm/day), resulting in 143 major landslides.

The climate was moderate, with temperatures ranging between 15°C and 30°C. During summer (March to May), temperatures can reach up to 35°C, whereas in winter (December to February), temperatures can drop to 10°C in elevated region. The highest peak, Anamudi, is 2,695 m high and contributes to a variety of microclimates and ecosystems. The Idukki Dam, a double-curvature arch dam on the Periyar River, is the tallest arch dam in Asia at 169 m. It has a reservoir capacity of 2,000 million cubic meters and is crucial for hydroelectric power generation and irrigation, as well as being a popular tourist destination. The overall workflow adopted in this study is summarized in the flowchart depicted in Figure 2.

Materials and methods

This study integrated multiple datasets shown in Table 1 to assess the influence of land use and land cover (LULC) changes on landslide susceptibility (Putra et al., 2025) Landslide inventory data were obtained from Bhukosh -Geological Survey of India (Badapalli et al., 2025) and the NASA Cooperative Open Online Landslide Repository (COOLR), which together provide a reliable database of past landslide occurrences in the study region (P et al., 2025).

Conditioning factors

Nineteen conditioning factors that affect slope instability were selected, reflecting both environmental and anthropogenic factors (Zhang et al., 2024). Topographic variables derived from a Digital Elevation Model (DEM) include Elevation, Slope, and Aspect, which directly affect slope stability; curvature parameters**,** such as profile curvature, which control flow convergence and divergence; Relief Amplitude and Slope Classes, representing terrain variability; and topographic indices, including the Topographic Wetness Index (TWI), Topographic Position Index (TPI), Terrain Ruggedness Index (TRI), Stream Transport Index (STI), and Stream Power Index (SPI), which describe hydrological flow, terrain roughness, and erosive power(Mondal & Mandal, 2017). Geological layers, soil maps, drainage density, and rainfall distribution were also integrated, as they critically influence landslide processes (Pourghasemi et al., 2013). Distance-to-road and distance-to-stream layers derived from OSM data were included to capture the anthropogenic and hydrological effects on slope stability.

Landslide susceptibility mapping

A Frequency Ratio (FR) model was adopted to evaluate the spatial relationship between landslide occurrences and conditioning factors (Moayedi et al., 2019). The FR method calculates the likelihood of landslide occurrence within each class of a conditioning factor (Hafsa et al., 2022) by comparing the proportion of landslide pixels to the proportion of area pixels in that class. This statistical approach provides a robust and interpretable framework for susceptibility (Ali et al., 2025) mapping, particularly in data-limited environments (Małka, 2021; Pradhan, 2010; Razavizadeh et al., 2017). The FR model is a geo-spatial calculation tool used to estimate the probabilistic association between the distribution of landslides and each of their conditioning factors (Equation 1) (He et al., 2023; Remondo et al., 2005).

$$FR = \frac{(N_{Landslide})}{(N_{Domain})} \qquad (1)$$

where is the percentage of landslide events located in each subclass and is the percentage of the class covered by it.

Scenario-based assessment

Two susceptibility maps were generated: one using the LULC from 2021 and the other using the projected LULC for 2050. All other conditioning factors were held constant to isolate the effects of land cover change on landslide susceptibility (Badapalli et al., 2025). The outputs were normalized and classified into susceptibility categories (Alqadhi et al., 2023) (very low, low, moderate, high, and very high). A comparative analysis of the two scenarios was conducted to identify areas likely to transition into higher susceptibility classes owing to anticipated land cover changes (Baig et al., 2022; Jalayer et al., 2022).

Results and discussion

Land use and land cover changes (2021–2050)

The LULC analysis revealed considerable changes between 2021 and 2050 (Table 3). The most striking transformation was the expansion of built-up areas, which increased from 355.22 km² in 2021 to 578.68 km² in 2050, representing a net gain of 223.46 km². This growth reflects accelerated urbanization, driven by population increases and developmental pressures on valley regions and slope foot zones.

Conversely, natural cover exhibited a decline (Figure 5). Tree cover decreased by 56.33 km², whereas bare ground decreased substantially by 161.19 km². Croplands, flooded vegetation, and water bodies showed marginal reductions of –1.47 km², –0.39 km², and –4.03 km², respectively. These declines, particularly in forested areas, are ecologically significant because vegetation plays a crucial role in stabilizing slopes through root reinforcement and hydrological regulation. The conversion of bare ground and tree cover into impervious surfaces explains the observed surge in the built-up area. Overall, the transition pattern suggests a landscape undergoing rapid human modification at the cost of natural buffers, which has direct implications for slope instability in the area.

Landslide susceptibility mapping (2021 vs 2050)

The frequency ratio model integrated with conditioning factors produced Landslide Susceptibility Maps (LSM) for 2021 and 2050. Geomorphological features like denudational hills and valleys, which dominate Idukki's landscape, amplify risks when combined with steep slopes (>25°), Anthropogenic pressures, such as road expansions and LULC conversions, further destabilize these zones by introducing surcharge loads and reducing vegetation cover, diminishing root reinforcement. The classification results (Table 4) highlighted a major redistribution of the susceptibility classes over the study period. In 2021, the susceptibility was dominated by the low (29.31%) and medium (27.33%) categories, which accounted for more than half of the study area. Very high susceptibility zones were relatively limited (6.22%). By 2050, the scenario shifts

dramatically: the very high susceptibility class expands to 32.20%, representing a 26% increase, whereas the very low (–13.56%) and low (–10.02%) classes decline sharply shown in Figure 7. This change in the very high susceptibility class should be interpreted in the context of the FR model's predictive performance (e.g., AUC values of 0.73–0.93 in similar Western Ghats studies, aligning with our validation [AUC value 0.94] Figure 6 and the fixed classification thresholds (natural breaks method) applied consistently to both scenarios for comparability.

This redistribution implies that large tracts of land previously considered stable are likely to become highly vulnerable to slope failure in the coming decades due to climate change. The expansion of the high and very high classes aligns with projected land cover changes, particularly the conversion of forests and bare ground into built-up surfaces as evidenced by historical trends in Idukki where builtup increased significantly from forest and additional shifts from agriculture from 2005 to 2015 (Comptroller and Auditor General of India, 2021).

Linking LULC transitions with landslide susceptibility

The comparative results clearly demonstrated the strong influence of LULC transitions on landslide susceptibility. Forest decline and urban expansion are the dominant processes that shape these changes. Built-up expansion, often occurring on marginal and steep terrains, introduces new loading and surface runoff conditions that aggravate the potential for slope failure. Field observations confirm this, with local residents actively excavating steep slopes for road side shops(Figure 3). Driven instead by tourism investments, labor in-migration for plantations and land conversions from unproductive agriculture/forests due to economic crises. Simultaneously, the reduction in tree cover diminishes natural slope reinforcement, further increasing susceptibility. The observed increase of 223.46 km² in the built-up area closely corresponds with the 26% rise in very high susceptibility zones, suggesting a direct causal relationship. The contraction of the low and very low susceptibility classes by more than 23% indicates that safer zones are being rapidly transformed into hazard-prone areas.

Table 1. Data sets used in the Landslide Susceptibility Mapping

S.No	Data	Description	Sources
1	ASTER DEM (30m)	Elevation, SPI, STI, TWI, TPI, Slope Aspect, Roughness, Slope classes, Profile Curvature, TRI, Relief Amplitude	https://search.earthdata.nasa.gov
2	Landsat 8 (30m)	Using Landsat OLI/ TIRS bands NDVI (Path & Row: 143, 54 Date: 08/10/2021, Path & Row: 144, 53 Date: 24/11/2021)	https://earthexplorer.usgs.gov
3	LU/LC	ESRI	https://livingatlas.arcgis.com/landcoverexplorer/
4	Lithology, Geomorphology, Lineamen	Digital lithology, Geomorphology, and Lineament thematic maps	https://bhukosh.gsi.gov.in/Bhukosh/MapViewer.aspx

5	Open Series Map (OSM)	Open street map	https://www.openstreetmap.org/
6	Rainfall	Gridded Rainfall data for the annual year 2021 (0.25 X 0.25 Degrees)	https://www.imdpune.gov.in/Clim_Pred_LRF_New/Grided_Data_Download.html

Table 2. LULC change detection from 2020-2021

S.No.	Change_detection (2020-2021)	Area_change (sq.km)
1	Water - Water	112.25
2	Water - Trees	2.88
3	Water - Flodded Vegetation	0.24
4	Water - Crops	0.17
5	Water - Built area	0.30
6	Water - Bare Ground	2.58
7	Trees - Water	1.86
8	Trees - Trees	3387.91
9	Trees - Flooded Vegetation	0.61
10	Trees - Crops	3.40
11	Trees - Built area	36.21
12	Trees - Bare Ground	97.24
13	Flooded vegetation - Water	1.90
14	Flooded vegetation - Trees	0.68
15	Flooded vegetation - Flooded Vegetation	3.17
16	Flooded vegetation - Built area	0.00
17	Flooded vegetation - Bare Ground	0.34
18	Crops - Water	0.02
19	Crops - Trees	6.23
20	Crops - Crops	24.01
21	Crops - Built area	0.83
22	Crops - Bare Ground	6.51
23	Built area - Water	0.21
24	Built area - Trees	37.58
25	Built area - Flooded Vegetation	0.00
26	Built area - Crops	1.48
27	Built area - Built area	312.12
28	Built area - Bare Ground	7.99
29	Bare Ground - Water	0.60
30	Bare Ground - Trees	97.24
31	Bare Ground - Flooded Vegetation	0.03
32	Bare Ground - Crops	6.27
33	Bare Ground - Built area	3.79
34	Bare Ground - Bare Ground	846.58

Table 3. LULC changes of existing year (2021), and projected year (2050)

Classes	Area (km^2)		Temporal changes(km^2) Increase(+)or Decrease(-)
	2021	2050	2050 – 2021
Water	116.80	112.76	-4.03
Trees	3528.39	3472.06	-56.33
Flooded Vegetation	4.09	3.70	-0.39
Crops	35.63	34.16	-1.47
Built Area	355.22	578.68	+223.46
Bare ground	964.38	803.19	-161.19

Table 4. Percentage of area under different susceptibility zones

Susceptibility level	LSM_2021(%)	LSM_2050(%)	% Changes
Very Low	19.24	5.68	-13.56
Low	29.31	19.28	-10.03
Medium	27.33	22.85	-4.48
High	17.90	19.98	2.08
Very High	6.22	32.20	25.98

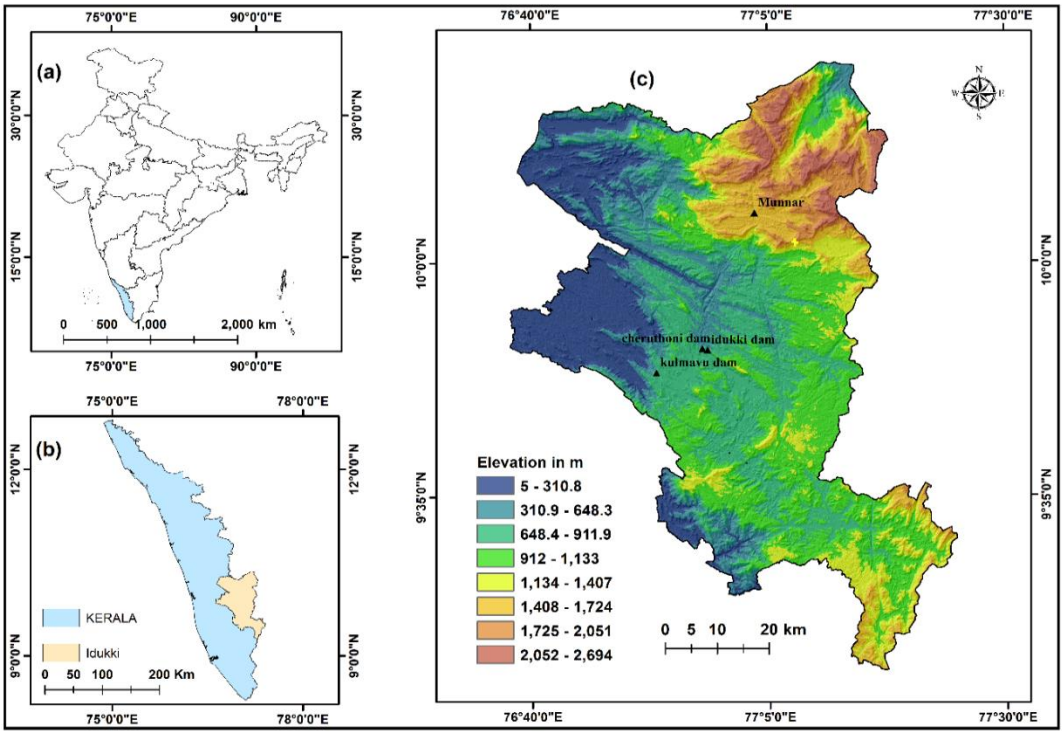

Figure 1. Location Map of the study area: (a) India (b) Kerala (c) Idukki

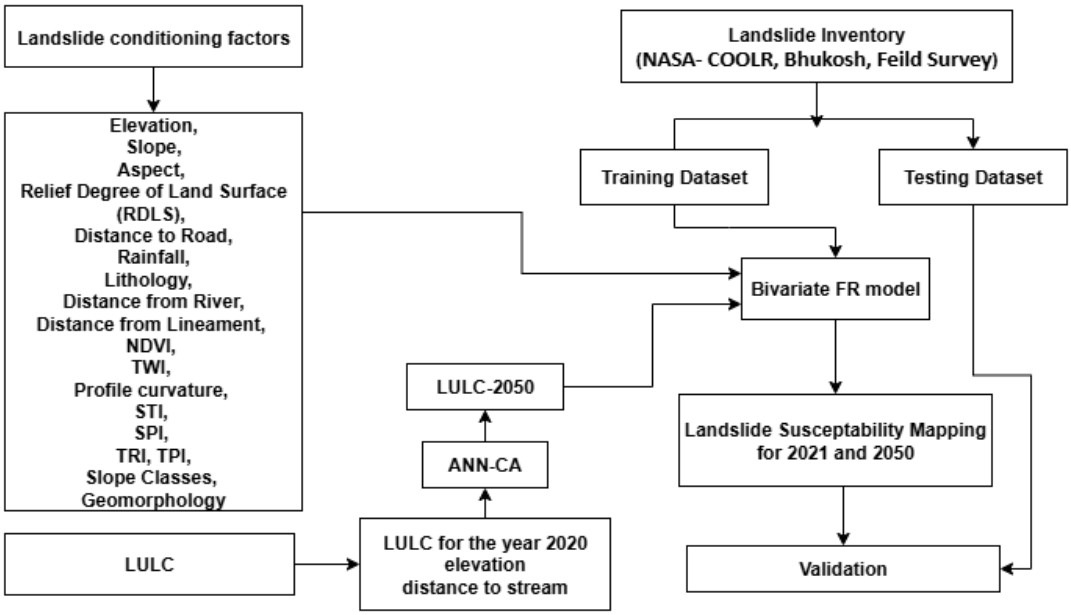

Figure 2. Methodology flowchart for LSM integrating 2021-2050 LULC Projections in Idukki district

Figure 3. Field observations of slope instability and anthropogenic slope modification in Idukki District, Kerala

© 2026, e-ISSN 2682-7727 https://doi.org/10.17576/geo-2026-2202-02

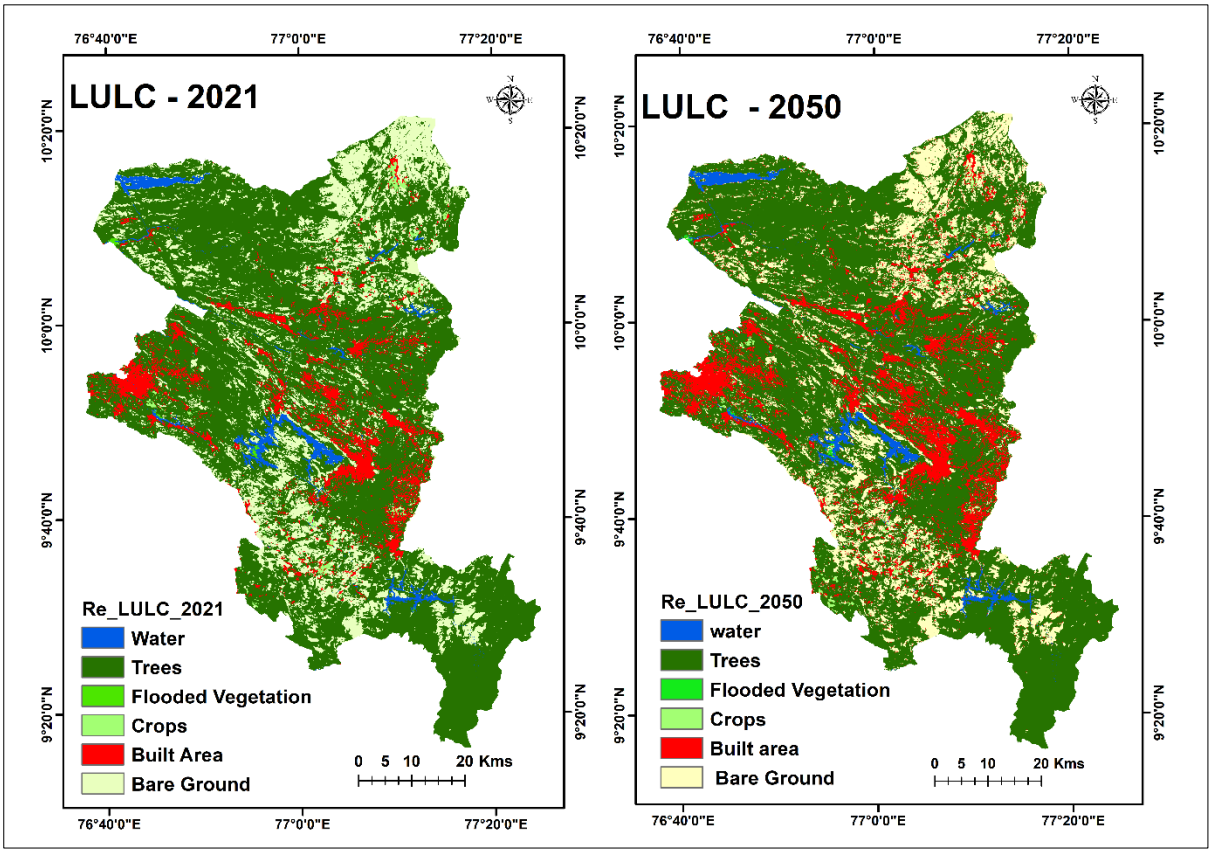

Figure 4. LULC maps of the year 2021 and 2050

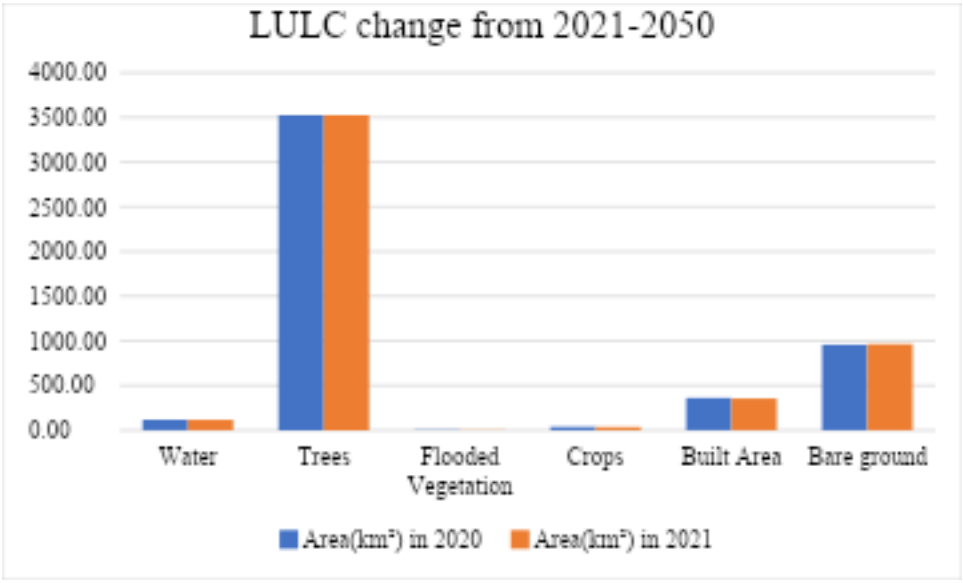

Figure 5. LULC changes from 2021 to 2050

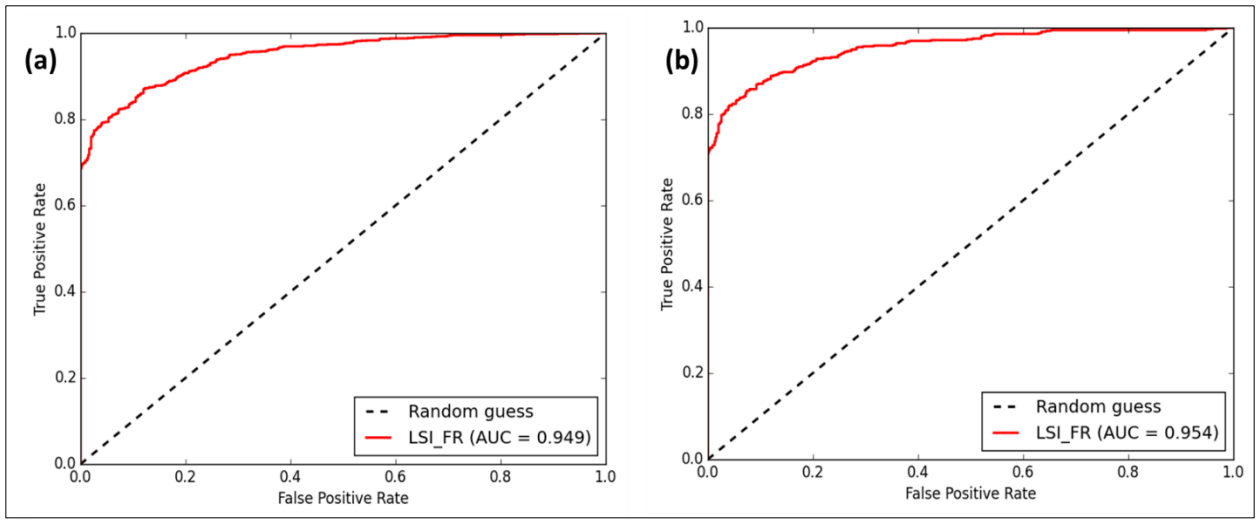

Figure 6. The success and prediction rate for landslide susceptibility map; (a) Success rate (b) Prediction rate

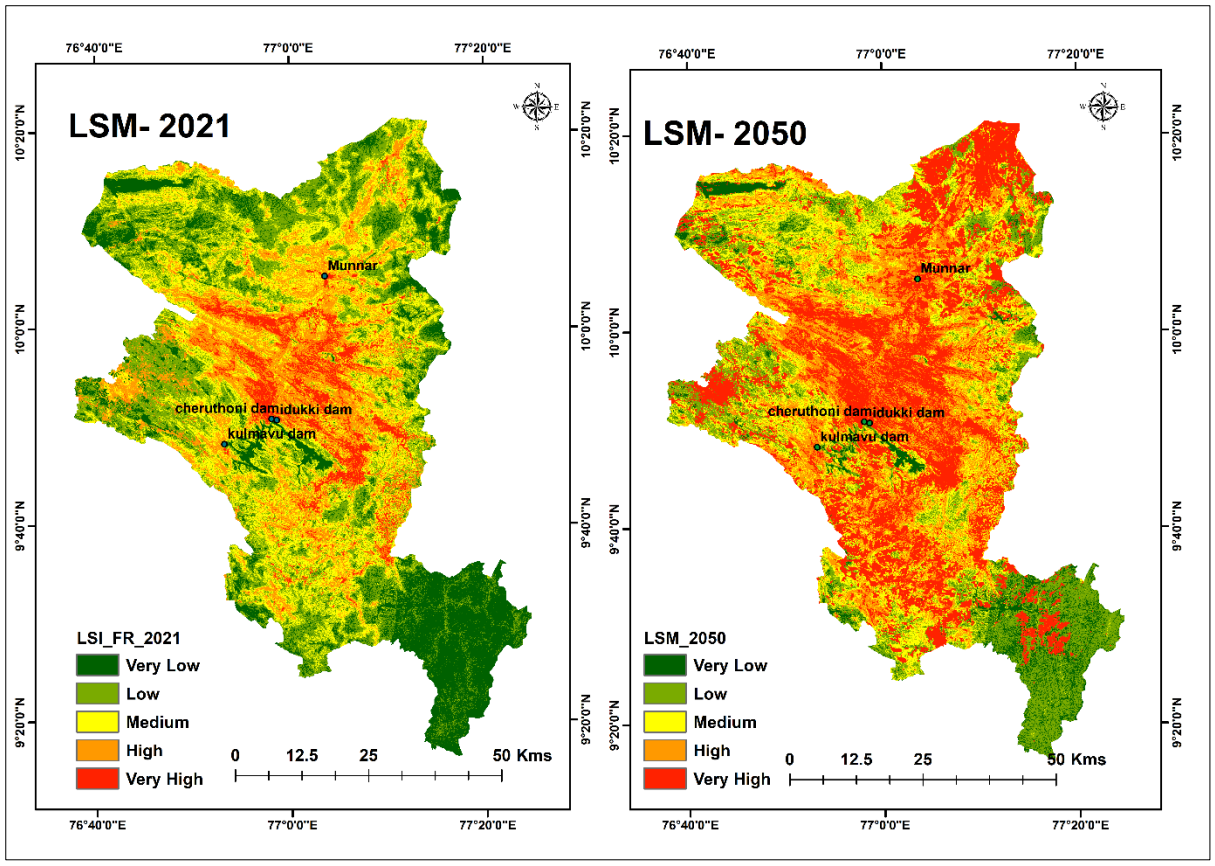

Figure 7. Landslide susceptibility maps of year 2021 and 2050

Conclusions

This study assessed the impact of land use and land cover (LULC) changes on landslide susceptibility by comparing the conditions in 2021 with projected scenarios for 2050. By integrating Frequency Ratio (FR) modeling with future LULC scenarios, the research highlights the escalating risks driven by anthropogenic pressures, such as urban expansion and forest degradation, which undermine natural slope stability through reduced root reinforcement and increased runoff. The results underscore that future urban development, if not properly managed, will significantly increase landslide risks. Integrating LULC change models with susceptibility mapping provides a powerful tool for anticipating hazard trends and guiding sustainable land management in landslide prone ecosystem. However, the study has limitations that warrant consideration. The FR model's reliance on historical landslide inventories for calibration assumes stationarity in factor relationships, which may not fully account for accelerating climate influences like intensified monsoons or extreme events. Additionally, LULC projections depend on scenario assumptions (e.g., CA-Markov), potentially underestimating uncertainties from socioeconomic variables or data resolution. Validation was limited to present-day conditions, as future landslides are unavailable, introducing potential biases in long-term predictions. Future work could address these gaps by incorporating hyperparameter tuning for the ANN component to enhance model precision, integrating dynamic climate variables.

References

Abraham, M. T., Pothuraju, D., & Satyam, N. (2019). Rainfall thresholds for prediction of landslides in Idukki, India: An Empirical approach. *Water*, *11*(10), 2113.

Achu, A. L., Joseph, S., Aju, C. D., & Mathai, J. (2021). Preliminary analysis of a catastrophic landslide event on 6 August 2020 at Pettimudi, Kerala State, India. *Landslides*, *18*(4), 1459–1463.

Ajin, R. S., Saha, S., Saha, A., Biju, A., Costache, R., & Kuriakose, S. L. (2022). Enhancing the Accuracy of the REPTree by Integrating the Hybrid Ensemble Meta-Classifiers for modelling the landslide Susceptibility of Idukki District, South-western India. *Journal of the Indian Society of Remote Sensing*, *50*(11), 2245–2265.

Ali, A., Teku, D., Sisay, T., & Mihret, B. (2025). Geospatial modeling of landslide susceptibility in Debek, South Wollo, Ethiopia: Comparative analysis of frequency ratio and analytical hierarchy process models for geohazards management. *Frontiers in Earth Science*, *13*, 1557860.

Alqadhi, S., Mallick, J., Hang, H. T., Al Asmari, A. F. S., & Kumari, R. (2023). Evaluating the influence of road construction on landslide susceptibility in Saudi Arabia's mountainous terrain: A bayesian-optimised deep learning approach with attention mechanism and sensitivity analysis. *Environmental Science and Pollution Research*, *31*(2), 3169–3194.

Anchima, S. J., Gokul, A., Senan, C. P. C., Danumah, J. H., Saha, S., Sajinkumar, K. S., Rajaneesh, A., Johny, A., Mammen, P. C., & Ajin, R. S. (2023). Vulnerability evaluation utilizing AHP and an ensemble model in a few landslide-prone areas of the Western Ghats, India. *Environment, Development and Sustainability*, *27*(3), 6423–6466.

Badapalli, P. K., Nakkala, A. B., Kottala, R. B., Gugulothu, S., Hasher, F. F. B., Mishra, V. N., & Zhran, M. (2025). Landslide susceptibility level mapping in Kozhikode, Kerala, using

machine learning-based Random Forest, Remote Sensing, and GIS techniques. *Land*, *14*(7), 1453.

Baig, M. F., Mustafa, M. R. U., Baig, I., Takaijudin, H. B., & Zeshan, M. T. (2022). Assessment of land use land cover changes and future predictions using CA-ANN simulation for Selangor, Malaysia. *Water*, *14*(3), 402.

Bernardie, S., Vandromme, R., Thiery, Y., Houet, T., Grémont, M., Masson, F., Grandjean, G., & Bouroullec, I. (2021). Modelling landslide hazards under global changes: The case of a Pyrenean Valley. *Natural Hazards and Earth System Sciences*, *21*(1), 147–169.

Bozzolan, E., Holcombe, E. A., Pianosi, F., Marchesini, I., Alvioli, M., & Wagener, T. (2023). A mechanistic approach to include climate change and unplanned urban sprawl in landslide susceptibility maps. *Science of The Total Environment*, *858*, 159412.

Chen, L., Guo, Z., Yin, K., Shrestha, D. P., & Jin, S. (2019). The influence of land use and land cover change on landslide susceptibility: A case study in Zhushan Town, Xuan'en County (Hubei, China). *Natural Hazards and Earth System Sciences*, *19*(10), 2207–2228.

Chitikela, N. V. L., & Kollipara, P. K. (2025). Geospatial-based assessment of land susceptibility mapping using the Bivariate Statistical Frequency Ratio Model: A case study of Idukki District, Kerala, India. *Disaster Advances*, *9*(18), 11.

Chowdhuri, I., Pal, S. C., Chakrabortty, R., Malik, S., Das, B., Roy, P., & Sen, K. (2021). Spatial prediction of landslide susceptibility using projected storm rainfall and land use in Himalayan region. *Bulletin of Engineering Geology and the Environment*, *80*(7), 5237–5258.

Dixit, A., Sahany, S., Rajagopalan, B., & Choubey, S. (2022). Role of changing land use and land cover (LULC) on the 2018 megafloods over Kerala, India. *Climate Research*, *89*, 1–14.

El Jazouli, A., Barakat, A., & Khellouk, R. (2019). GIS-multicriteria evaluation using AHP for landslide susceptibility mapping in Oum Er Rbia high basin (Morocco). *Geoenvironmental Disasters*, *6*(1), 3.

Froude, M. J., & Petley, D. N. (2018). Global fatal landslide occurrence from 2004 to 2016. *Natural Hazards and Earth System Sciences*, *18*(8), 2161–2181.

Guns, M., & Vanacker, V. (2013). Forest cover change trajectories and their impact on landslide occurrence in the tropical Andes. *Environmental Earth Sciences*, *70*(7), 2941–2952.

Hafsa, B., Chowdhury, Md. S., & Rahman, Md. N. (2022). Landslide susceptibility mapping of Rangamati District of Bangladesh using statistical and machine intelligence model. *Arabian Journal of Geosciences*, *15*(15), 1367.

He, L., Wu, X., He, Z., Xue, D., Luo, F., Bai, W., Kang, G., Chen, X., & Zhang, Y. (2023). Susceptibility assessment of landslides in the Loess Plateau based on machine learning models: A case study of Xining City. *Sustainability*, *15*(20), 14761.

Jacinth Jennifer, J., & Saravanan, S. (2022). Artificial neural network and sensitivity analysis in the landslide susceptibility mapping of Idukki district, India. *Geocarto International*, *37*(19), 5693–5715.

Jalayer, S., Sharifi, A., Abbasi-Moghadam, D., Tariq, A., & Qin, S. (2022). Modeling and predicting land use land cover spatiotemporal changes: A case study in Chalus Watershed, Iran. *IEEE Journal of Selected Topics in Applied Earth Observations and Remote Sensing*, *15*, 5496–5513.

Jones, S., Kasthurba, A. K., Bhagyanathan, A., & Binoy, B. V. (2021). Landslide susceptibility investigation for Idukki district of Kerala using regression analysis and machine learning. *Arabian Journal of Geosciences*, *14*(10), 838.

Laxmi, Ch. N. V., & Kumari, K. P. (2024). Evidential Belief Function (EBF) model for landslide susceptibility analysis in Idukki District, Kerala, India. *International Journal of Environment and Climate Change*, *14*(12), 464–472.

Leta, M. K., Demissie, T. A., & Tränckner, J. (2021). Hydrological responses of watershed to historical and future land use land cover change dynamics of Nashe Watershed, Ethiopia. *Water*, *13*(17), 2372.

Li, P., Wang, H., Li, H., Ni, Z., Deng, H., Sui, H., & Xu, G. (2024). Refined landslide susceptibility mapping considering land use changes and InSAR deformation: A case study of Yulin City, Guangxi. *Remote Sensing*, *16*(16), 3016.

Małka, A. (2021). Landslide susceptibility mapping of Gdynia using Geographic Information System-based statistical models. *Natural Hazards*, *107*(1), 639–674.

Martha, T. R., Roy, P., Khanna, K., Mrinalni, K., & Vinod Kumar, K. (2019). Landslides mapped using satellite data in the Western Ghats of India after excess rainfall during August 2018. *Current Science*, *117*(5), 804.

Moayedi, H., Osouli, A., Tien Bui, D., & Foong, L. K. (2019). Spatial landslide susceptibility assessment based on Novel Neural-Metaheuristic Geographic Information System based ensembles. *Sensors*, *19*(21), 4698.

Mondal, S., & Mandal, S. (2017). Application of Frequency Ratio (FR) model in spatial prediction of landslides in the Balason river basin, Darjeeling Himalaya. *Spatial Information Research*, *25*(3), 337–350.

Muñoz-Torrero Manchado, A., Antonio Ballesteros-Cánovas, J., Allen, S., & Stoffel, M. (2022). Deforestation controls landslide susceptibility in Far-Western Nepal. *CATENA*, *219*, 106627.

P, L., C, M., Mathew, A., & Shekar, P. R. (2025). Machine learning and deep learning-based landslide susceptibility mapping using geospatial techniques in Wayanad, Kerala state, India. *HydroResearch*, *8*, 113–126.

Pacheco Quevedo, R., Velastegui-Montoya, A., Montalván-Burbano, N., Morante-Carballo, F., Korup, O., & Daleles Rennó, C. (2023). Land use and land cover as a conditioning factor in landslide susceptibility: A literature review. *Landslides*, *20*(5), 967–982.

Pourghasemi, H. R., Pradhan, B., Gokceoglu, C., Mohammadi, M., & Moradi, H. R. (2013). Application of weights-of-evidence and certainty factor models and their comparison in landslide susceptibility mapping at Haraz watershed, Iran. *Arabian Journal of Geosciences*, *6*(7), 2351–2365.

Pradhan, B. (2010). Landslide susceptibility mapping of a catchment area using frequency ratio, fuzzy logic and multivariate logistic regression approaches. *Journal of the Indian Society of Remote Sensing*, *38*(2).

Putra, A. N., Jaenudin, Prasetya, N. R., Sugiarto, M. T., Sudarto, Prayogo, C., Maritimo, F., & Admajaya, F. T. (2025). Utilizing Remote Sensing and Random Forests to identify optimal land use scenarios and address the increase in landslide susceptibility. *Sustainability*, *17*(9), 4227.

Ramachandran, R. M., & Reddy, C. S. (2017). Monitoring of deforestation and land use changes (1925–2012) in Idukki district, Kerala, India using Remote Sensing and GIS. *Journal of the Indian Society of Remote Sensing*, *45*(1), 163–170.

Razavizadeh, S., Solaimani, K., Massironi, M., & Kavian, A. (2017). Mapping landslide susceptibility with frequency ratio, statistical index, and weights of evidence models: A case study in northern Iran. *Environmental Earth Sciences*, *76*(14), 499.

Remondo, J., Bonachea, J., & Cendrero, A. (2005). A statistical approach to landslide risk modelling at basin scale: From landslide susceptibility to quantitative risk assessment. *Landslides*, *2*(4), 321–328.

Roccati, A., Paliaga, G., Luino, F., Faccini, F., & Turconi, L. (2021). GIS-based landslide susceptibility mapping for land use planning and risk assessment. *Land*, *10*(2), 162.

Sharma, A., & Sandhu, H. A. S. (2024). Investigating the dynamic nature of landslide susceptibility in the Indian Himalayan region. *Environmental Monitoring and Assessment*, *196*(3), 257.

Suriyankietkaew, S., Krittayaruangroj, K., Thinthan, S., & Lumlongrut, S. (2025). Community capitals framework for sustainable development: A qualitative study of creative tourism in Ban Chiang World Heritage Site. *Sustainability*, *17*(8), 3311.

Tyagi, A., Tiwari, R. K., & James, N. (2023). Prediction of the future landslide susceptibility scenario based on LULC and climate projections. *Landslides*, *20*(9), 1837–1852.

Yono, A., Mokua, R. A., & Dube, T. (2025). Remote sensing of land cover change dynamics in mountainous catchments and semi-arid environments: A review. *Geocarto International*, *40*(1), 2476602.

Youssef, A. M., Mahdi, A. M., & Pourghasemi, H. R. (2022). Landslides and flood multi-hazard assessment using machine learning techniques. *Bulletin of Engineering Geology and the Environment*, *81*(9), 370.

Zhang, D., Jindal, D., Roy, N., Vangla, P., & Frost, J. D. (2024). Enhancing landslide susceptibility mapping using a positive-unlabeled machine learning approach: A case study in Chamoli, India. *Geoenvironmental Disasters*, *11*(1), 21.